Pinhole Imagery*

KAZUO SAYANAGI†
Institute of Optics, The University of Rochester, Rochester, N. Y. 14627
(Received 22 December 1966)

Pinhole imagery is discussed by using modulation transfer functions. The optimum condition between the size of the pinhole and the focus position is understood as the balance of the diffraction caused by the aperture size and the geometrical-optical aberration given by the aperture size and focus position. Field characteristics, chromatic characteristics and relations with receptor systems are discussed easily in the spatial-frequency domain.

INDEX HEADING: Image formation; Diffraction; Aberrations; Modulation transfer function.

THE pinhole has been used as an imaging device for centuries. The oldest description of pinhole imagery I could find was written by the Arabian scholar Ibn Al-Haithan (A.D. 965–1038). He pointed out that the finest imaging with the pinhole can be obtained by using a very small hole and discussed the image quality when the size and the shape of the hole are changed, as follows:

"The image of the sun only shows this property when the hole is very small. If the hole is larger the image changes, and the change is more marked with increasing size of the hole. If the hole is very large, the crescent shape of the image disappears altogether, and the light becomes round if the hole is round, quadrangular if it is quadrangular, and with any shaped opening you like, the image takes the same shape, always provided the hole is large and the receiving surface parallel to it."[1]

In the earliest stage of its history, the pinhole was used mainly for the observation of solar eclipses. Later, from the 15th century on, it was used in the so-called camera obscura. The quality of pinhole imagery then became more and more important.

The first physical consideration of this subject, based on a mixed treatment of geometrical and physical optics, was written by Petzval.[2] He expressed the diameter D of the image point made by the pinhole as the sum of the geometrical diameter d and the diameter of the diffraction pattern caused by the aperture d,

$$D=d+2l\lambda/d, \tag{1}$$

where l is the distance between the pinhole and the receiving plane and λ is the wavelength of the incident light. The optimum diameter of the hole is defined so as to give the minimum diameter of the point image. From

$$\partial D/\partial d=1-2l\lambda/d^2,$$

he obtained

$$d_p^2=2l\lambda, \tag{2}$$

where d_p is the optimum diameter of the pinhole, for which $\partial D/\partial d=0$.

Lord Rayleigh's analysis[3] was based on Fraunhofer diffraction in the presence of defocus; he calculated point spread functions for different pinhole diameters. Comparing the calculated diameters of point images with several photos taken with the same conditions, he concluded that

$$d_R^2=3.6l\lambda. \tag{3}$$

This relation can be combined with another result in the form "the pinhole covers about nine-tenths of the first Fresnel zone."

Selwyn recently discussed the same problem[4] using the central intensity of the normalized point spread function and found the relation

$$d_s^2=3l\lambda. \tag{4}$$

His consideration was not limited to axial imagery as in previous cases, but extended to off-axial imagery. He pointed out that "off-axial imagery suffers from chromatic aberration, curvature of field, and a form of astigmatism."

We can find many different rules in textbooks of optics such as the result of Petzval,[5] Rayleigh's result[6] and its comparison with the Fresnel zone,[7] Selwyn's result,[8] another independently obtained relation (constant of Eqs. (2)~(4) is 2.56)[9] and an experimental

---

* Part of this work was done by the author when he was at the Institute of Optical Research, Stockholm, supported by the Swedish National Science Research Council and was presented at ICO in München, 20–25 August 1962.

† On leave of absence from the Canon Camera Co., Inc., Tokyo.

[1] H. Gernsheim, *The History of Photography* (Oxford University Press, New York, 1955), p. 1.

[2] J. Petzval, Wien Ber. **XXVI**, 33 (1857); Phil. Mag. **XVII**, 1 (1859).

[3] Lord Rayleigh, Phil. Mag. **XXXI**, 87 (1891); *Sci. Paper* Vol. I (Dover Publications, New York, 1965), p. 513.

[4] E. W. H. Selwyn, Phot. Z. **90B**, 47 (1950).

[5] For example, A. C. Hardy and F. H. Perrin, *The Principles of Optics* (McGraw-Hill Book Company, Inc., New York, 1932), p. 124.

[6] For example, R. W. Wood, *Physical Optics* (Macmillan Company, New York, 1934), 3rd ed., p. 270.

[7] For example, J. M. Stone, *Radiation and Optics* (McGraw-Hill Book Company, Inc., New York, 1963), p. 204.

[8] For example, R. Kingslake, *Lenses in Photography* (A. S. Barnes and Company, Inc., New York, 1963), Rev. ed., p. 60.

[9] For example, J. Flügge, *Das Photographische Objektiv* (Springer-Verlag, Wien, 1955), p. 8.

table.[10] Practical applications of the pinhole appear even in modern optical instrumentation.[11] It is therefore desirable to clarify the concepts of pinhole imagery.

Optical imagery in the presence of defocus was discussed by Hopkins[12] and Steel[13] recently, using modulation transfer functions. This new tool for image analysis opens the way for further discussion of the pinhole problem.

Some results of this approach to pinhole photography are described in this paper. The optimum relation between the pinhole diameter and the focal length can differ according to the image-evaluation criteria. Field and chromatic characteristics of pinhole imagery may be discussed using a criterion based on wave-optical transfer functions, and with an extension of the method full-field and heterochromatic imagery can be included. It is also possible to include the effects of the receptor on the optimization.

RELATIONS

In this section we consider only a circular aperture and incoherent illumination. The wavefront coming from an object point at infinity can be considered as a plane wave; the distance between this plane wave and a reference sphere having its center at the image point shown in Fig. 1 is defined as the wavefront aberration and is given approximately by the form,

$$W(\xi,\eta)=a_{20}(\xi^2+\eta^2), \tag{5}$$

where ξ and η are the normalized coordinates in the pinhole; the pinhole diameter is d; the distance between the center of the pinhole and assumed axial image point is l. The aberration coefficient is easily obtained by geometrical considerations, approximately

$$a_{20}=d^2/8l, \tag{6}$$

when the object is at infinity, and

$$a_{20}=d^2(a+l)/8al, \tag{6'}$$

when the object is at the distance a from the pinhole and d is very small compared with a and l.

It is convenient to introduce a parameter μ,

$$\mu=\pi d^2/4\lambda l, \tag{7}$$

which shows directly the amount of the wavefront aberration in units of wavelength. Using the new expression we get,

$$l=\pi d^2/4\lambda\mu, \tag{8}$$

and

$$d^2=(4\mu/\pi)\lambda l. \tag{9}$$

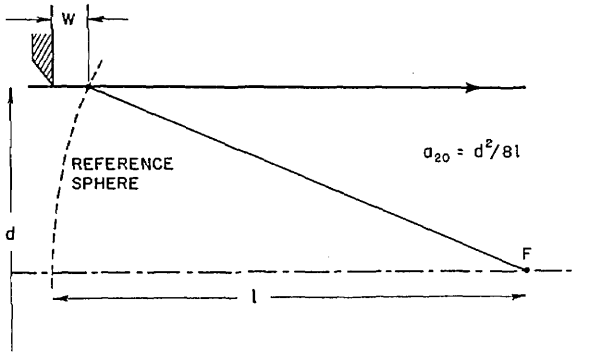

FIG. 1. Geometrical scheme of pinhole.

The F number of the pinhole is given by

$$F=l/d=\pi d/4\lambda\mu. \tag{10}$$

The theoretical cut off frequency of the modulation transfer function for given F number is given approximately by[12]

$$u_c=2\sin\alpha/\lambda=4\mu/\pi d=d/\lambda l, \tag{11}$$

where $\sin\alpha$ is the numerical aperture of the pinhole.

A table of numerical values of the modulation transfer function in the presence of defocus is given by Steel[13] for each value of μ up to 14. The parameter μ was introduced for the purpose of using this table.

The quality of the image made by the pinhole is represented precisely by the modulation transfer function. Sometimes, however, it is difficult to judge the relative quality of two transfer functions having different forms. It is therefore desirable to introduce a single figure of merit derived from the transfer curves. As measures of the merit of image quality we can use integrated values of the modulation transfer function such as,

$$Q_{II}=\int_{-\infty}^{\infty}\int T(u,v)\,du\,dv, \tag{12}$$

the two-dimensional figure of merit and

$$\left.\begin{aligned} Q_{Ix}&=\int_{-\infty}^{\infty} T(u,o)\,du,\\ Q_{Iy}&=\int_{-\infty}^{\infty} T(o,v)\,dv, \end{aligned}\right\} \tag{13}$$

as one-dimensional figures of merit. Here u, v are orthogonal spatial frequencies and are characteristic of radial and tangential imagery, respectively. $T(u,v)$ is the normalized modulation transfer function. By using the integral theorem of Fourier transforms we

[10] W. Merte, R. Richter, and M. V. Rohr, *Das Photographische Objektiv* (Verlag von Julius Springer, Wien, 1932), p. 17.
[11] A. H. Gallas, C. A. Gilbert, and A. B. Hitterdal, J. Soc. Motion Picture Television Engrs. 74, 321 (1965). P. A. Newman and V. E. Rible, Appl. Opt. 5, 1225 (1966).
[12] H. H. Hopkins, Proc. Phys. Soc. (London) A231, 91 (1955).
[13] W. H. Steel, Opt. Acta 3, 65 (1956).

can describe each figure of merit by[14]

$$Q_{II}=t(0,0), \tag{12'}$$

$$\left.\begin{aligned} Q_{Ix}&=h_x(0)\\ Q_{Iy}&=h_y(0)\end{aligned}\right\}, \tag{13'}$$

where

$$t(x,y)=\int_{-\infty}^{\infty}\int T(u,v)\exp\{-2\pi i(ux+vy)\}dudv, \tag{14}$$

and

$$\left.\begin{aligned} h_x(x)&=\int_{-\infty}^{\infty}t(x,y)dy,\\ h_y(y)&=\int_{-\infty}^{\infty}t(x,y)dx\end{aligned}\right\}. \tag{15}$$

$t(x,y)$ is called the point spread function, $h_x(x)$ and $h_y(y)$ are the line spread functions for radial and tangential imagery, respectively. Our figures of merit are interpreted as the central intensity of the point or line spread function and, therefore, could be considered equivalent to the extended Strehl definition.[15]

The central intensity of the point spread function in the presence of defocusing is given by[16]

$$I=\left(\frac{\pi d^2A}{4\lambda f^2}\right)^2\left[\frac{\sin(U/4)}{U/4}\right]^2, \tag{16}$$

where

$$U=(2\pi/\lambda)(d/2f)^2Z, \tag{17}$$

f is the focal length of the lens, A is the amplitude of the light in the pupil (uniform all over the pupil), and Z is the longitudinal defocus. In our case, f equals l. Using the relation[17]

$$a_{20}=-\tfrac{1}{2}(d/2f)^2Z \tag{18}$$

and Eqs. (6) and (7), we get

$$I=4A^2/l^2[\sin(\pi d^2/8\lambda l)]^2. \tag{19}$$

Equation (19) is the result when we have an amplitude A in the pupil, but for the normalized modulation transfer function we have the condition

$$\int_{-\infty}^{\infty}\int t(x,y)dxdy=1. \tag{20}$$

For our case the amplitude A must have the value which satisfies Eq. (20). From

$$(\pi d^2/4)A^2=1,$$

we get

$$A^2=4/\pi d^2. \tag{21}$$

Substituting Eq. (21) into Eq. (19), we can get

$$Q_{II}=16/\pi d^2l^2[\sin(\pi d^2/8\lambda l)]^2. \tag{22}$$

For the case of Q_I, we do not have any such analytical expression. We must calculate it numerically from the modulation transfer curves for each specific case.

OPTIMUM APERTURE SIZE AND FOCUS POSITION

Equation (22) is given as a function of d and l. Therefore we can get two different conditions for the optimization of merit with respect to d and l, respectively.

We first discuss the effect of the diameter change for the fixed-focus position. From

$$\frac{\partial Q_{II}}{\partial d}=\frac{8}{\pi d^2l^2}\left(\sin\frac{\pi d^2}{8\lambda l}\right)\left\{\frac{\pi d}{\lambda l}\cos\frac{\pi d^2}{8\lambda l}-\frac{4}{d}\sin\frac{\pi d^2}{8\lambda l}\right\}=0,$$

we get

$$\tan(\pi d^2/8\lambda l)=\pi d^2/4\lambda l,$$

then from Eq. (7),

$$\mu\doteqdot 0.742\pi\doteqdot 2.331. \tag{23}$$

The optimum condition is expressed by using Eq. (9) as

$$d_{Q_{II}}{}^2=2.968\lambda l. \tag{24}$$

This result is the same as Selwyn's,[4] because he was using the same criterion. One-dimensional results are obtained by numerical calculation,

$$\mu\doteqdot 2.2, \tag{25}$$

and

$$d_{Q_I}{}^2=2.7\lambda l. \tag{26}$$

The effect of focus change for the fixed pinhole can be obtained in the same way from

$$\frac{\partial Q_{II}}{\partial l}=-\frac{32}{\pi d^2l^3}\left(\sin\frac{\pi d^2}{8\lambda l}\right)\left\{\sin\frac{\pi d^2}{8\lambda l}+\frac{\pi d^2}{8\lambda l}\cos\frac{\pi d^2}{8\lambda l}\right\}=0;$$

we get

$$\tan(\pi d^2/8\lambda l)=-\pi d^2/8\lambda l,$$

then

$$\mu\doteqdot 1.292\pi\doteqdot 4.056. \tag{27}$$

The optimum condition is written as

$$d^2=5.168\lambda l_{Q_{II}}, \tag{28}$$

or

$$l_{Q_{II}}=d^2/5.168\lambda. \tag{28'}$$

[14] K. Sayanagi, Oyo Butsuri **25**, 193 (1956).
[15] K. Strehl, Z. Instrumentenk. **15**, 362 (1895).
[16] M. Born and E. Wolf, *Principles of Optics* (Pergamon Press, Inc., New York, 1965), 3rd ed., p. 440 and 441.
[17] H. H. Hopkins, *Wave Theory of Aberration* (Clarendon Press, Oxford, 1950), p. 16.

TABLE I. k value of the optimum condition $d^2=k\lambda l$ by different authors. ($k=4\mu/\pi$)

Author		k	
Petzval[2]		2	
Rayleigh[3]		3.6	
Selwyn[4]		3	
Sayanagi	given l	3.0	2.7
	given d	5.2	3.8
		two-dimension	one-dimension

The one-dimensional condition in this case is also given by numerical calculation as

$$\mu \doteqdot 3.0, \tag{29}$$

and

$$d^2=3.8\lambda l_{Q_I}, \tag{30}$$

or

$$l_{Q_I}=d^2/3.8\lambda. \tag{30'}$$

The results, and those of other authors are summarized in Table I, using the constant k in the optimum condition

$$d^2=k\lambda l, \tag{31}$$

where

$$k=4\mu/\pi. \tag{31'}$$

Our four results are different from each other and also from the results given by three authors.

Figures 2 and 3 show the modulation transfer functions in the case of diameter change and focus-position change, respectively. The wavefront aberration μ is chosen as the parameter in each figure.

The reason for an optimum combination of pinhole diameter and focus position can be clarified by using the concepts of diffraction and aberration.

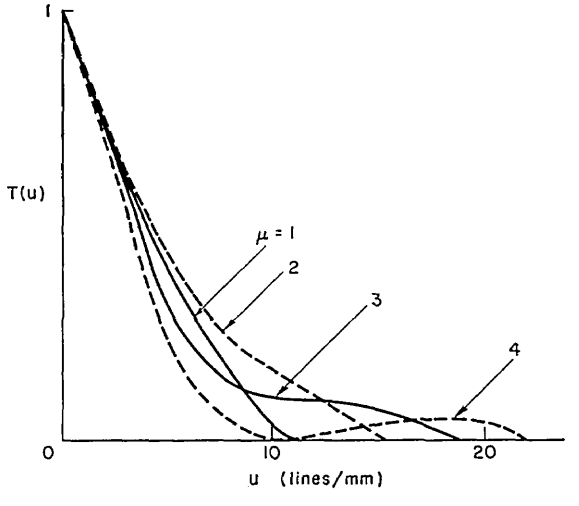

FIG. 2. Modulation transfer functions for varying pinhole. Diameter $l=20.9$ mm, $\lambda=500$ mμ and

$\mu=1$	$l=0.12$ mm
2	0.16
3	0.20
4	0.23.

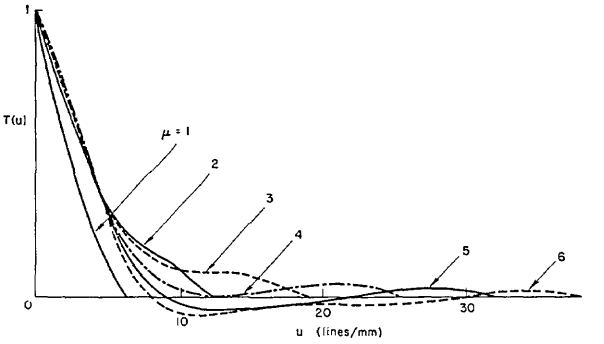

FIG. 3. Modulation transfer functions for varying focus. Position $d=0.20$ mm. $\lambda=500$ mμ and

$\mu=1$	$l=62.8$ mm
2	31.4
3	20.9
4	15.7
5	12.6
6	10.5.

Let us consider the diameter change. When the diameter is small, the theoretical cutoff caused by diffraction is small and the amount of the defocus aberration is also small. Therefore the shape of the modulation transfer function for small μ (see $\mu=1$) is almost the same as the case of the aberration-free aperture, that is to say, the modulation-transfer factor decreases almost linearly with spatial frequency up to the theoretical cutoff. Increasing the diameter of the pinhole results in a higher theoretical cutoff and also a larger amount of aberration, which, according to Eq. (6), is proportional to the square of the diameter. Because of this aberration, the modulation transfer function for the larger aperture decreases in the lower-frequency region and becomes lower than the modulation transfer factor for the small μ (see $\mu=3$ and 4 as compared with $\mu=1$), even though the theoretical cutoff is larger. The modulation transfer function for the small aperture is diffraction limited. The large aperture is aberration limited. Our optimum condition occurs between these two extremes as the balance of diffraction and aberration.

The same phenomena are observed in Fig. 3. The modulation transfer function in the case of a short focal length (large value of μ) has its cutoff in the high-frequency domain because of the relatively large numerical aperture, but the modulation transfer factor in the lower-frequency region is low and sometimes negative because of the large amount of the aberration. On the other hand, in the case of a long focal length, we get a high modulation transfer factor in the low frequency region but low cutoff frequencies because of the small numerical aperture. In this case, however, the balancing point is different than the aperture change. This difference can be understood from the different change of diffraction and aberration with respect to the diameter and the focus position. According to Eq. (6), aperture varies as the square, and the

focus position inversely with the amount of aberration, but according to Eq. (10), the aperture varies linearly and inversely with the theoretical cutoff frequency. That is to say, in the case of the diameter change, the increase of aberration is larger than the increase of spread caused by focus-position change for the same cutoff frequency, and therefore, the balance occurs at a smaller value of μ than for the case of the focus-position change.

Other differences appear between the two-dimensional and one-dimensional results. Dependence of these merit functions on the slope of spread functions (therefore also on the slope of optical transfer functions) has been pointed out.[14] In general, aberrant spread functions have relatively higher two-dimensional figures of merit than have aberration-free ones because of the flare which spreads out around the core. The results for the two-dimensional merit function are therefore higher than those of the one-dimensional case. For example, in the case of the focus-point change, we can see in Fig. 3 that the modulation transfer functions for $\mu=3$ and 4 are quite different from each other and that the former gives a one-dimensional maximum and the latter a two-dimensional maximum. This results because the two-dimensional figure of merit is proportional to u^2, while the one-dimensional figure of merit is proportional to u. The same situation can be observed in the case of the diameter change. In my opinion, the one-dimensional merit defined by Eq. (13) is more useful for general imaging processes.

If we change the focus position, the imaging magnification for the object at the finite distance is also changed. Therefore, it is necessary to introduce a relative spatial frequency in object space. This problem will be discussed later.

RESOLVING POWER

Change of the theoretical cutoff frequency is given by Eq. (11) and is directly proportional to the diameter of the pinhole and reciprocally proportional to the focus position. As shown by Figs. 2 and 3, the real cutoff frequencies for the higher values of μ are lower than the theoretical ones because of the effect of the large amount of the defocus aberration.

In Fig. 4, the changes of the theoretical cutoff, the geometrical cutoff[18] and the real cutoff frequency with respect to the pinhole diameter change are summarized from Fig. 2. In addition, the cutoff frequency defined from the value of modulation transfer function at 0.05 is given in Fig. 4. In the smaller-diameter region, we expect higher resolution from the geometrical-optical point of view, but diffraction results in lower resolution. In the larger-diameter region, the real cutoff frequency converges with the geometrical one because of the

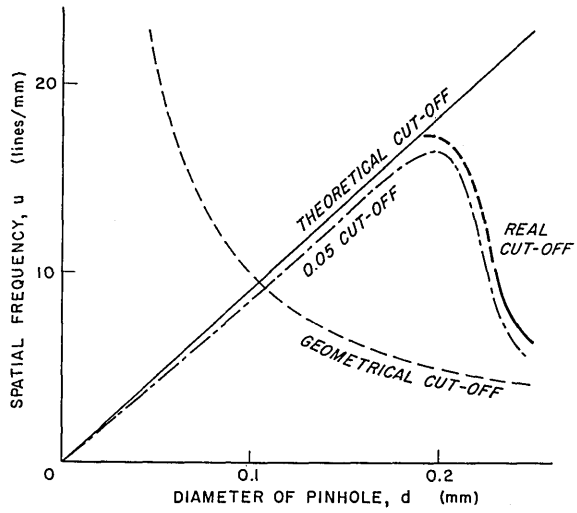

FIG. 4. Field characteristics of optimum focus position;
———— radial image plane,
- - - - - - tangential image plane.

increasing defocus aberration[19] in spite of the higher theoretical cutoff frequency. Between these two regions, we have an interesting diameter at which the real resolution is higher than the geometrical-optical one and is the same as the theoretical cutoff. The maximum real resolution occurs when $\mu=3$ (then the diameter is 0.2 mm) and is about 3.2 times the geometrical-optical one.

From Fig. 3, we can get the same result. The maximum resolution for the case of the focus position change is also at $\mu=3$ (then the focus position is 20.9 mm for 0.2 mm diameter) and the value is about 3.2 times the geometrical-optical one as shown in Fig. 5.

Considerations in this section showed that the optimum for maximum resolution is $\mu=3$ (approximately) in both cases.

FIELD CHARACTERISTICS

The apparent aperture shape as viewed from an off-axial image point is oval. The diffraction theory of aberration for oval-shaped apertures is, in general, very difficult to evaluate. The modulation transfer functions for the case of defocus, however, can be obtained easily.

The modulation transfer function[20] is

$$T(s)=(1/A)\int\int_p \exp[iksW(\xi,\eta;s)]d\xi d\eta \quad (32)$$

for a normalized spatial frequency s, where A is the area of the aperture, p indicates the common area of the two shifted apertures and $W(\xi\cdot\eta;s)$ is

$$W(\xi,\eta;s)=(1/s)[W(\xi+\tfrac{1}{2}s,\eta)-W(\xi-\tfrac{1}{2}s,\eta)]$$

[18] Assuming that the spread function is the uniform disk.

[19] H. H. Hopkins, Proc. Roy. Soc. (London) **A231**, 91 (1955).
[20] H. H. Hopkins, Proc. Phys. Soc. (London) **B70**, 449 (1957).

from the wavefront aberration $W(\xi,\eta)$. In the case of defocus aberration, by using Eq. (5) and expansion of each, we get

$$W(\xi,\eta;s)=2a_{20}\xi, \tag{33}$$

and also for

$$T(t)=(1/A)\int\int_p \exp[iktW(\xi,\eta;t)]d\xi d\eta, \tag{32'}$$

and

$$W(\xi,\eta;t)=(1/t)[W(\xi,\eta+\tfrac{1}{2}t)-W(\xi;\eta-\tfrac{1}{2}t)],$$

we get

$$W(\xi,\eta;t)=2a_{20}\eta. \tag{33'}$$

Equations (32) and (32') are the modulation transfer functions for the x and y directions, respectively, and as shown by Eqs. (33) or (33') each function in the integration is a function of only one variable. Therefore, our oval-shaped aperture can be replaced with the circular aperture of which the radius is different for the radial and tangential cases. For the radial case, we can consider the diameter of the pinhole as

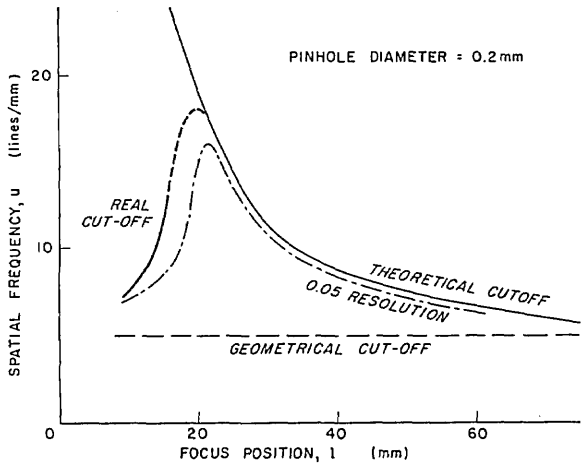

FIG. 5. Resolving power for diameter change. Focus position 20.9 mm, $\lambda=500$ mμ.

$$\left.\begin{aligned} d_r&=d,\\ \text{and}\qquad d_t&=d\cos\theta \end{aligned}\right\} \tag{34}$$

for the tangential case, where θ is the field angle.

When these effective apertures are known, by using Eq. (8), we can get the optimum distance from the pinhole to the focus point for any given μ value. Then, the distances of the focal planes are given as

$$\left.\begin{aligned} l_r&=(\pi d_r^2/4\lambda\mu)\cos\theta=(\pi d^2/4\lambda\mu)\cos\theta,\\ l_t&=(\pi d_t^2/4\lambda\mu)\cos\theta=(\pi d^2/4\lambda\mu)\cos^3\theta. \end{aligned}\right\} \tag{35}$$

These equations show a kind of astigmatism and field curvature of the pinhole. In the case of symmetrical optical systems such aberrations are given as the result of ray refraction by spherical (or any other) surfaces; but in our pinhole problem the cause of aberration-like phenomena is the change of the apparent aperture and the balance between aberration (only defocus) and diffraction. This field characteristic is illustrated in Fig. 6. The solid line shows the radial image plane and the dotted line the tangential.

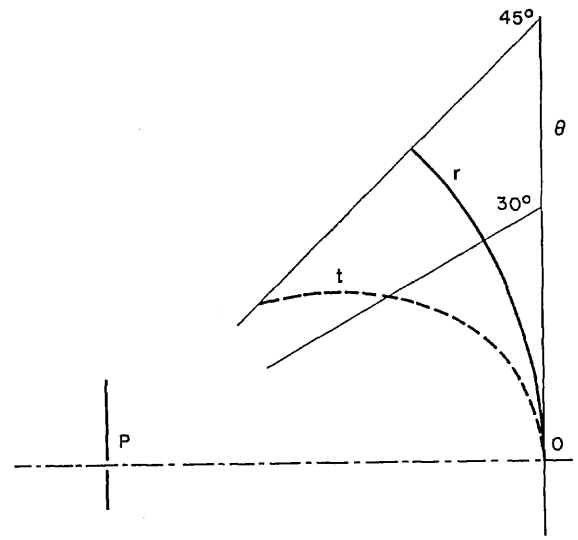

FIG. 6. Resolving power for focus position change. Diameter 0.2 mm, $\lambda=500$ mμ.

The theoretical cutoff frequency of the modulation transfer function at each optimum condition can be calculated for both azimuths by using Eqs. (11) and (34),

$$u_{cr}=4\mu/\pi d_r=4\mu/\pi d \tag{36}$$

$$u_{ct}=4\mu/\pi d_t=4\mu/\pi d\cos\theta. \tag{37}$$

The result for the tangential image is given for the plane which is perpendicular to the off-axial ray; therefor the real cutoff in image plane, which is perpendicular to the optical axis, is given approximately by

$$u_{ct}'=(4\mu/\pi d\cos\theta)\cos\theta=4\mu/\pi d. \tag{38}$$

Equations (36) and (38) show that the cutoff frequency and therefore the shape of the modulation transfer functions is the same for each optimum-focus point.

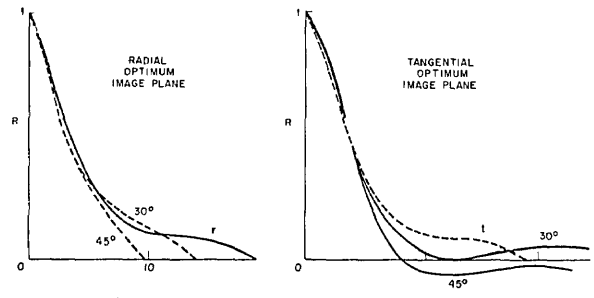

FIG. 7. Modulation transfer function at radial and tangential optimum image plane. $\mu=3$.

Examples of the modulation transfer function are given in Fig. 7, which shows the modulation transfer functions at the radial and tangential optimum image plane, respectively. We can easily see that the radial and tangential modulation transfer functions at each optimum image plane are the same and also that the tangential image is diffraction-limited in the radial plane and that the radial image is aberration-limited in the tangential plane. The modulation transfer functions illustrated in Fig. 7 clearly show the physical figure of the field characteristics based on the balance between aberration and diffraction.

Star images for each focus point at $\theta=30°$ are shown in Fig. 8. The image at the radial-image plane has relatively simple oval diffraction pattern because in this case the imagery for both azimuths is diffraction-limited. The image at the tangential-image plane shows very special structure. It has simple structure at the tangential section (horizontal in the figure) but outside maxima at the radial section because of the large amount of defocus aberration for radial imagery, which has been discussed before.

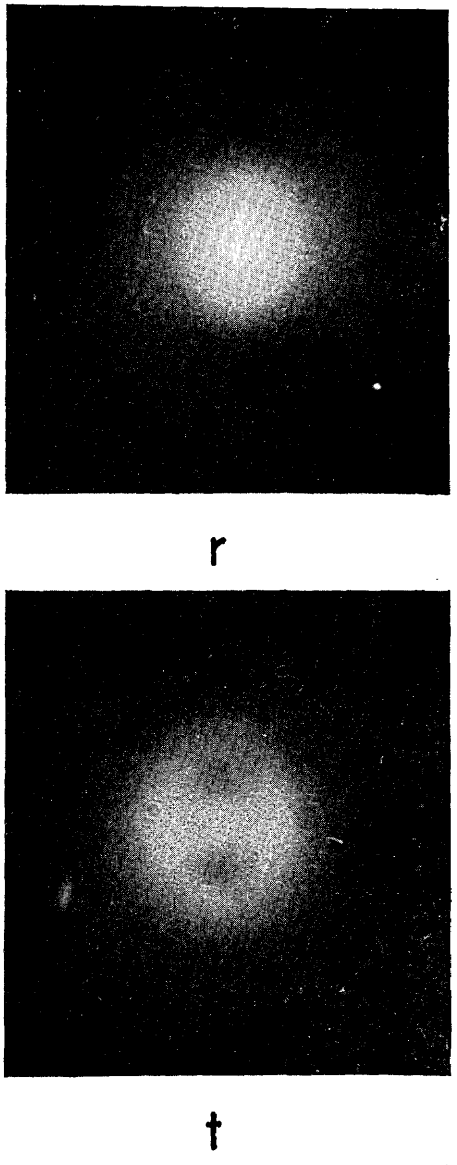

FIG. 8. Diffraction pattern at radial and tangential optimum image plane. $\mu=3$.

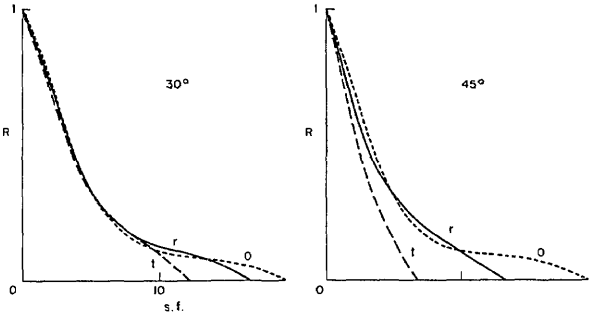

FIG. 9. Off-axial modulation transfer function for the image plane of $\mu=3$ at on-axis.

Figure 9 shows modulation transfer functions for the image plane at the on-axis condition of $\mu=3$.

CHROMATIC CHARACTERISTICS

The relations discussed in the previous section are functions of the wavelength λ. For example, the equations

$$\mu=\pi d^2/4\lambda l$$

and

$$u_c=d/\lambda l$$

show that the amount of aberration and the theoretical cutoff frequency are proportional to the wave number $1/\lambda$.

Furthermore, we can get the optimum condition for the wavelength by taking the derivative of Q_{II} with respect to λ as follows,

$$\partial Q_{II}/\partial\lambda=-(4/\lambda^2 l^3)\sin(\pi d^2/8\lambda l)\cos(\pi d^2/8\lambda l)=0$$

then

$$\pi d^2/8\lambda l=\pi/2.$$

We can rewrite the above condition as

$$\mu_{cII}=\pi d^2/4\lambda l=\pi \tag{39}$$

and

$$d^2=4\lambda l. \tag{40}$$

These results show that, if we take $\mu=\pi$ (therefore $k=4$) for the optimum aperture size or focus position, the chromatic characteristics take the maximum at the wavelength used for the design. This is another optimum condition.

In the case of the one-dimensional figure of merit we get the following results by numerical calculation:

$$\mu_{cI}=3.0 \tag{41}$$

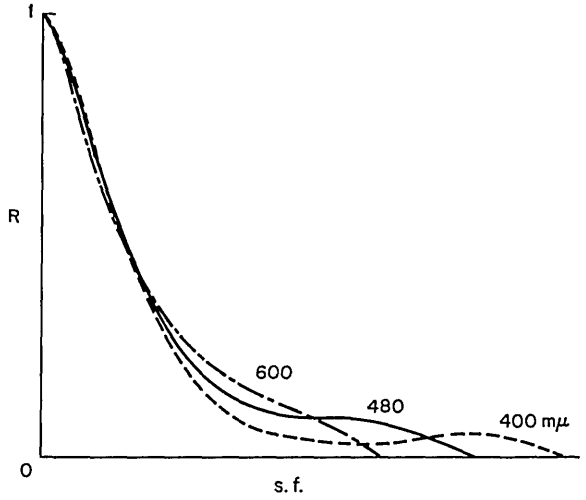

FIG. 10. Chromatic difference of modulation transfer function when $\mu=3$ for 480 mμ.

and

$$d^2=3.8\lambda l. \tag{42}$$

This is not so different from the two-dimensional condition.

For an example, we take $\mu=3$ at the middle wave number ($\lambda=480.0$ $m\mu$) between 400 and 600 $m\mu$ in Fig. 10. In this case, the change of curves is not so significant compared with the diameter or focus-point change. The curves are almost similar in the low-frequency region; their cutoffs are different from each other but occur in the less important region where the other curves take very low values.

Therefore, we can say that chromatic characteristics are not so important in practical applications if we take the middle wavenumber as the design point. The loss in the one-dimensional figure of merit for both extreme wavelengths, 400 and 700 mμ, is only 5% compared to the middle wavenumber.

If we are using c times conditions (39) and (41) depending upon dimensional choice, from

$$\mu=\pi d/4\lambda l=c\mu_c, \tag{43}$$

we get

$$\mu_c=\pi d^2/4(c\lambda)l=\pi d^2/4\lambda' l, \tag{44}$$

where $\lambda'=c\lambda$. Equation (44) shows that chromatic characteristics are best at the wavelength λ' which is c times the wavelength used in the design.

RELATION WITH RECEPTORS

Behavior of receptors such as photographic films can also be treated by using the modulation transfer functions. Usually, receptors have the character of so-called low-pass filters, and the optimum condition of the pinhole might differ from the results we discussed in previous sections because of weighting according to frequency.

In the case of the closed-circuit TV for example, the combined system of the image tube (vidicon) and electronic transmitter has a cutoff frequency of 18.4 lines/mm, which corresponds to 4.73 Mc in audio frequency. Then only the frequency region below 18.4 lines/mm is of interest and the optimum values of μ or k are slightly lower than the values obtained in the previous section from the shapes of the modulation transfer functions illustrated in Fig. 2.

Our discussions in the previous sections are based on the spatial frequency at the focus position; it is different for the fixed-focus position. In the case of the focus-position change however, there is a magnification change due to the focal length. Then, if we discuss the spatial frequency at unit distance in the object space, the theoretical cutoff is given by Eq. (11) as

$$u_c'=u_c\cdot l=d/\lambda. \tag{45}$$

It is constant for a fixed pinhole diameter; a longer focal position gives a better modulation transfer function because of smaller defocus aberration. The loss of illuminance in the image plane which comes from a small relative aperture is, however, disastrous, because of the combination of such a small aperture with a great focal distance. The question of the optimum diameter arises again, to improve the image quality and illuminance.

Zweig *et al.*[21] and Jones[22] pointed out that the informational sensitivity or the quantum efficiency of photographic films are almost the same for different sensitometric speeds. In other words, necessary exposure in the image and square of the resolution have a kind of reciprocity, such as

$$(\text{exposure}\times\text{resolution})_{\text{film}}=\text{const.} \tag{46}$$

We can also find the same kind of situation for pinhole imagery. Illuminance of the image can be considered reciprocally proportional to the squared F number of the pinhole (Eq. 10) as

$$\text{illuminance of the image} \propto 1/F=16\lambda^2\mu^2/\pi^2d^2, \tag{47}$$

and the resolution in the above sense is reciprocally proportional to the square of the theoretical cutoff frequency, then

$$\text{resolution in the image} \propto (1/\mu_c^2)=\pi^2d^2/16\mu^2. \tag{48}$$

Product of the above two quantities shows

$$(\text{illuminance}\times\text{resolution}) \propto \lambda^2=\text{const.} \tag{49}$$

This also shows a reciprocity between illuminance and resolution.

Combinations of the pinhole and photographic materials, both obeying laws of reciprocity, give the same

[21] H. J. Zweig, G. C. Higgins, and D. L. MacAdam, J. Opt. Soc. Am. 48, 926 (1958).
[22] R. C. Jones, J. Opt. Soc. Am. 51, 1159 (1961).

image quality in the sense that enlarged prints from the different combinations under the same exposure time (for negatives) to the same size of object in the final print carry almost the same information from the object.

From the above point of view, an extra-high-sensitivity material such as, Royal–X,[21,22] can be used for pinhole photography in combination with a larger aperture to get maximum information from the object. Therefore, considerations of informational sensitivity for different photosensitive materials or transducers are important to the application of pinhole imagery in practical uses.

SUMMARY

By using modulation transfer function analysis, we can discuss almost the whole subject of pinhole imagery. As was pointed out in the introduction, pinhole imagery was previously studied in a classical manner but a remarkable advance can be obtained by our approach.

The optimum condition, the main problem in this paper, was examined from different but necessary viewpoints, say two- and one-dimensional modulation transfer functions, resolving power, field characteristics, chromatic characteristics, and receptors. Our results are summarized in Table II. Among them, the value for field characteristics and receptors shows only the direction to be taken to maximize the average, for example, with respect to the whole field angle. It is necessary to evaluate the value of k or μ for each given field angle or receptor in each case. From this table, we can use the condition $k=3.8$, which is not so different from Lord Rayleigh's result $k=3.6$ for general purposes. The importance of the informational sensitivity of the receptor is pointed out; recent rapid advances of opto-electric transducers will give future applications of the pinhole to practical instruments.

TABLE II. k value of the optimum condition $d^2=k\lambda l$ for different conditions.

$(k=4\mu/\pi)$

Condition	Given l	Given d
Two-dimensional merit	3.0	5.2
One-dimensional merit	2.7	3.8
Resolving power	3.8	
Field characteristics	larger value on axis	
Chromatic characteristics	4.0	3.8
Receptors	smaller value for low pass filter	

ACKNOWLEDGMENT

The author is indebted to Dr. L. O. Hendeberg for his kind help on the experiments.